

# Performance of rocket data communication system using wire rope isolator on sounding rocket RX

Kandi Rahardiyanti<sup>1</sup>, Shandi Prio Laksono<sup>2</sup>, Khaula Nurul Hakim<sup>3</sup>, Yuniarto Wimbo Nugroho<sup>1</sup>,  
Andreas Prasetya Adi<sup>4</sup>, Salman<sup>5</sup>, Kurdianto<sup>6</sup>

<sup>1</sup>Research Center of Rocket Technology, National Research and Innovation Agency (BRIN), Bogor, Indonesia

<sup>2</sup>Research Center of Energy Conversion and Conservation, National Research and Innovation Agency (BRIN),  
South Tangerang, Indonesia

<sup>3</sup>Research Center of Electronics, National Research and Innovation Agency (BRIN), South Tangerang, Indonesia

<sup>4</sup>Research Center of Aeronautics Technology, National Research and Innovation Agency (BRIN), Bogor, Indonesia

<sup>5</sup>Ammunition Product Development Department, PT. Pindad, Bandung, Indonesia

<sup>6</sup>Research Center of Geoinformatics, National Research and Innovation Agency (BRIN), Bogor, Indonesia

## Article Info

### Article history:

Received Apr 23, 2024

Revised Nov 4, 2024

Accepted Nov 11, 2024

### Keywords:

Acceleration

Inertial measurement unit

Rocket

Vibration

Wire rope isolator

## ABSTRACT

The rocket experiment (RX) ballistic rocket requires a reliable data communication system capable of withstanding intense vibrations and shocks during flight. This study investigates the application of wire rope isolators (WRI) to damper mechanical disturbances and protect the rocket's communication system. Installation of WRI position and direction in this experiment with compression position. A series of vibration tests were conducted using 4 WRI installed in the rocket's 30 kg data communication compartment, vibration test results frequency between 4 Hz and 1500 Hz with acceleration of 8.37 g to 20.37 g, higher "g" readings on the test object sensor compared to vibration machine readings are usually caused by phenomena such as resonance, differences in dynamic response, non-linear behavior, sensor placement location, and swing effects when the vibration machine oscillates. This is a natural mechanical response to external vibrations during testing. While the results of flight tests rocket RX has an acceleration of 8 g to 9.3 g. The results showed that the WRI dampers are effective in protecting the data communication system and ensuring the uninterrupted transmission of flight data to the ground control station (GCS).

*This is an open access article under the [CC BY-SA](https://creativecommons.org/licenses/by-sa/4.0/) license.*



## Corresponding Author:

Kandi Rahardiyanti

Research Center of Rocket Technology, National Research and Innovation Agency (BRIN)

Mekarsari No.2, Bogor, Indonesia

Email: kand001@brin.go.id

## 1. INTRODUCTION

Ballistic rocket technology or rocket experiment (RX) developed by the National Research and Innovation Agency (BRIN), this rocket has a diameter of 450 mm. The data communication system of the RX ballistic rocket consists of a microcontroller, a 6-degree of freedom (DOF) inertial measurement unit (IMU) sensor, a radio transceiver, switching cables, and a power supply. For the safety and stability of the rocket during flight, the data communication system is crucial. It collects and analyzes data on temperature, speed, and altitude, which helps to enhance the dynamics and overall performance of the rocket [1]. The 6-DOF sensor includes an accelerometer and a gyroscope. The micro electro mechanical system (MEMS) accelerometer measures acceleration by converting the acceleration of an object into an electrical signal. This electrical signal is then detected by the accelerometer. Due to its compact size and high accuracy compared to conventional types, this device is widely used in industries such as aviation, automotive, and

seismic surveying [2]–[6]. The MEMS type significantly broadens application scenarios because it offers substantial advantages in integration and intelligence compared to conventional accelerometers. In most cases, MEMS accelerometers are categorized into piezoresistive, capacitive, piezoelectric, and other categories [7]–[10]. One of the most widely used MEMS accelerometers operates as a piezoresistive semiconductor.

The RX rocket flight tests have experienced several failures. One example of its failure is when the rocket's data communication system failed to transmit the required data to the ground control station (GCS). Many sources of dynamic loads occur during flight tests in the frequency range 5 and 200 Hz [11]. In addition, shocks caused by various rocket behaviors during flight tests can lead to vibrations with a wide range of frequencies [12], [13]. Therefore, significant efforts are made to protect the data communication system from vibrations and shocks, especially during rocket launch. The RX ballistic rocket, which is large and long, is designed as an atmospheric research rocket. A rocket with a high aspect ratio requires a wide bandwidth frequency range and reliable control. Therefore, a well-functioning damper is necessary to ensure that the rocket's control operates correctly [14].

Rocket development has improved the thrust-to-weight ratio and length-to-diameter ratio, which are crucial for long-range flight. Due to the thrust forces present during the rocket's initial launch, significant vibrations and shocks occur. Desmond *et al.* found that directional stability can be enhanced by optimizing the size and location of concentrated masses [15]. In rocket design, one crucial element that must be considered is vibration [16], [17]. This is especially relevant for rockets with high acceleration and high initial thrust. Various methods are used to study and analyze vibrations and shocks to predict the impact on the structure and equipment. Many vibrations are unavoidable but remain within tolerable limits [18]. Negative effects such as fatigue, noise, and wear can be caused by mechanical shocks. For example, military, naval, aerospace, and transportation applications require protection for sensitive electronic devices [19], [20].

To reduce shocks and vibrations, absorption systems can be implemented to protect the rocket's data communication system from acceleration forces, shocks, and vibrations throughout the rocket's trajectory [21]. Leblouba *et al.* [22] state that, essentially, vibration isolation systems are devices designed to minimize vibrations. This technology aims to reduce the propagation and transmission of energy, creating a safer and more comfortable environment. In situations where vibrations become intolerable, an analysis of the system's response to vibration effects and enhancement of mechanical properties are required, or the addition of isolation systems to counteract vibrations if improving mechanical properties is not feasible in the system design. To implement vibration isolation systems, it is essential to understand the components involved in vibration control, which include the source, path, and receiver of vibrations.

Dal and Baklaci [23] mention that vibration isolators are widely used to protect sensitive machinery, such as electronic devices and military equipment, from destructive shocks and vibrations. In the past several years, various equipment has been designed to protect structures from unwanted vibrations and to reduce those vibrations. Ramirez *et al.* [24] indicate that, for the purpose of isolating vibrations and shocks, flexible supports and/or effective mass increase of the system are commonly employed to lower the natural frequencies of the isolated system. Ferdek and Dukala [25] highlighted that wire rope isolators (WRI) are frequently used to eliminate vibrations from various sources, such as flight systems, sensitive electronics, and building structures.

The type of device marketed as an excellent shock isolator is the WRI, also known as a cable isolator. WRI is made by twisting strands of steel around a core strand, and the resulting wire rope can be modified to create a spring. WRI is capable of storing and dissipating compact and high amounts of energy. The stiffness characteristics of the wire rope are nonlinear due to its configuration. To protect sensitive equipment in aerospace and mechanical engineering, WRIs control vibrations and shocks through their geometric and mechanical properties [26]. Specifically, WRIs are superior to ordinary linear isolators in isolating shock vibrations under certain operational conditions, such as with low-frequency sinusoidal input [27] and pulses with high amplitude and long duration [28]. WRIs can dissipate significant amounts of energy, regardless of the shape of the wire rope, whether it is helical, circular, or curved. This is due to their damping properties, which depend on the size, number of strands, and diameter of the wire rope. Furthermore, the direction of loading—shear, roll, and axial—affects the behavior of the WRI [29], [30].

Stainless steel WRIs are one of the best types of vibration isolators for both vibration and shock isolation. For this reason, WRIs are widely used in industrial applications. WRIs are commonly used to minimize vibration and shock during the transportation of military equipment. The protection of sensitive electronic devices from shock involves WRIs consisting of holders and wires made from various materials; the final WRI is formed by attaching the wire between two holders aligned with one another. During active operation, relative movement occurs between the strands forming the wire. Due to the friction between each strand, WRIs exhibit nonlinear characteristics. Because of their damping performance, WRIs are widely used.

WRIs provide flexibility in all directions due to the friction and sliding between the intertwined wires. As a result, they function as friction-type dampers, utilizing stranded wire as the elastic component and Coulomb damping between the individual wire strands. Helical WRIs are used for heavy equipment applications while polycal WRIs are mainly used for mechanical and micro-electronic applications. As the length of the supporting wire increases and the natural frequency decreases, high-mode vibrations are more likely to occur [31].

The objective of this research is to experimentally analyze the damping capabilities of the WRI in the RX ballistic rocket to reduce the vibrations and shocks that occur during flight, ensuring that the data communication system can transmit the necessary data to GCS for analyzing the flight characteristics of the RX rocket. The research also aims to assess the effectiveness of the 4 WRIs installed in the RX rocket’s large and heavy data communication compartment (30 kg) in damping vibrations and shocks during launch. Success in obtaining the rocket’s acceleration data during the initial launch phase could lead to flight tests with larger and longer rockets, equipped with WRIs as vibration and shock dampers.

**2. METHOD**

The data communication system, which is part of the rocket’s payload, encompasses various disciplines and technologies. The complexity of the rocket’s data communication system presents challenges in multiple aspects, such as safety, reliability, and performance. The development of the data communication system employs various techniques to enhance its performance and reliability, including propulsion, thermal management, integrated modular avionics, the use of advanced materials and composites, computer science, and aerospace engineering [32]–[34]. Consequently, safety analysis, optimization, and reliability engineering are critical to ensuring that the data communication system operates safely and efficiently [35]–[38]. Electronic instruments within this system enable several vital tasks, such as communication, navigation, flight control, data processing, and vehicle management [39]. The rocket’s data communication system is designed to be miniaturized and standardized [40].

The method applied in this research involves creating a data communication system equipped with WRI dampers, enabling the system to withstand vibrations of up to 8 g and 15 g. Before conducting flight tests, vibration tests were carried out to ensure that the data communication system, equipped with WRI vibration dampers, could accurately record acceleration data and that the system itself would function effectively under vibration conditions. Figure 1 illustrates the process flow for testing the performance of the data communication system under vibration during both vibration testing and flight testing.

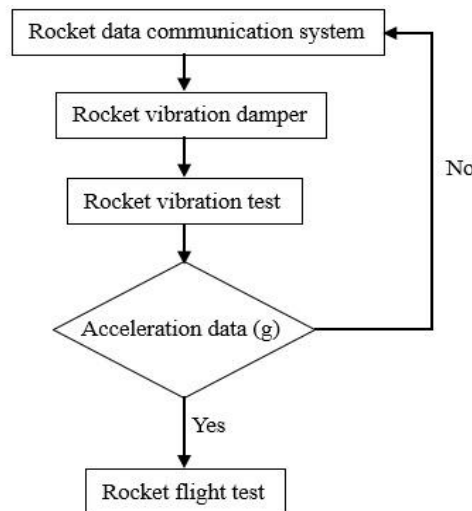


Figure 1. The process flow for testing the performance of the data communication system under vibration

**2.1. Rocket data communication system**

The rocket’s data communication system, consisting of a 6-DOF IMU with accelerometer and gyroscope sensors, is based on both the object and navigation coordinates. The IMU used in this research is the MPU9150 (accelerometer and gyroscope) and ADXL78 (accelerometer) [41]. Both are capable of

measuring acceleration between 4 g and 50 g. The accelerometer output is acceleration in meters per second squared, while the gyroscope output is angular velocity in radians per second.

For the data communication system to function and transmit acceleration and trajectory data to GCS, a power system is required. The power input to the system is direct current (DC), with a voltage of 7 volts, powering a 5 volt serial data circuit and a 3 volt sensor circuit. The output from this system is transmitted via a 5 volt radio transmitter, which operates at a frequency of 900 MHz and can communicate up to 100 km with a data rate of 345 kbps. The rocket data communication system weighs 30 kg. Figure 2 illustrates the system equipped with WRIs.

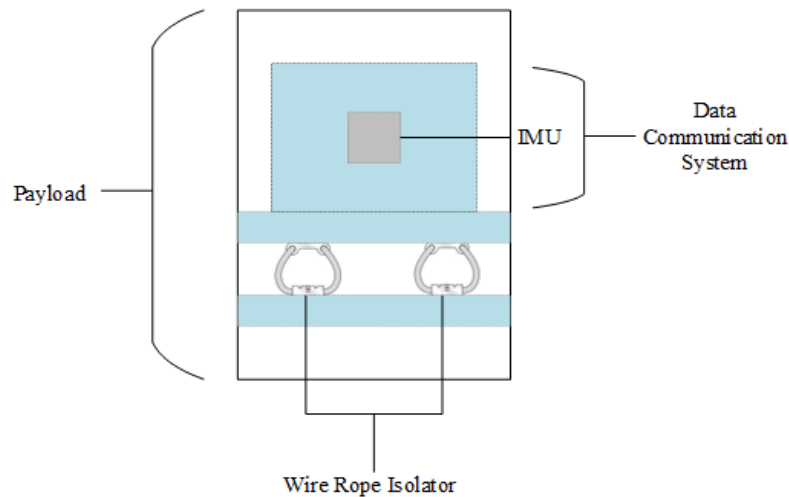


Figure 2. Rocket RX data communication system

## 2.2. Vibration damper

The rocket experiences vibrations during its launch, which will impact the data communication system. To minimize these vibrations, dampers are required and installed in the rocket's data communication system. A simple theory of wire rope states that wire rope is subject only to tensile, compressive, and torsional stresses, considering that the wire only experiences pure tensile forces while ignoring gripping conditions and contact stresses. It can be assumed that the frictional effects between the strands in a wire rope are minimal and can be neglected. The effective stiffness of the damper will decrease as the vibration amplitude increases, reaching a minimum value. The normal force and the angle change between the wire strands can be theoretically calculated when a mass ( $m$ ) impacts the wire rope at a certain velocity ( $v$ ) and spring stiffness ( $k$ ). Assuming  $x$  is the deformation due to compression and  $W$  is the axial load acting on the wire rope, then [42]:

$$\frac{1}{2}[mv]^2 = \frac{1}{2}[kx]^2 \quad (1)$$

$$W = kx \quad (2)$$

$$W = v\sqrt{mk} \quad (3)$$

Based on the installation position and the direction of the load axis acting on the damper, there are 4 types of mounting orientation as shown in Figure 3. The position and orientation of the compression WRI mounting axis are illustrated in Figure 3(a). Figure 3(b) displays the WRI mounting in the 45° compression/roll position. The sliding and fixed WRI mounting positions are shown in Figure 3(c), while Figure 3(d) depicts the fixed roll WRI position. The wire rope isolator used in this research is shown in Figure 4. A total of four units of wire rope isolator were installed in data communication system compartment, where they were subjected to compression loading, as shown in Figure 4(a). The dimensions of wire rope isolator are shown in Figure 4(b).

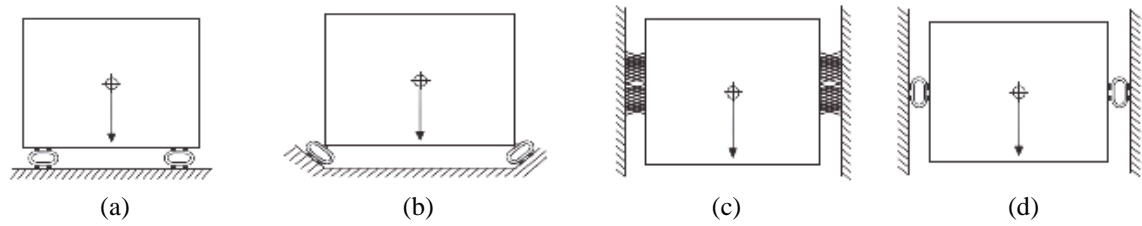
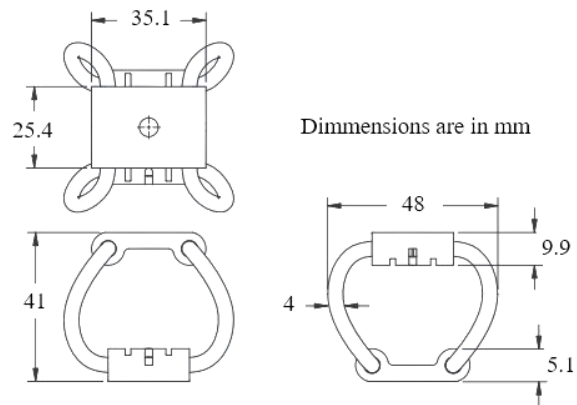


Figure 3. WRI mounting position (a) compression, (b) 45° compression/roll, (c) fixed shear, and (d) fixed roll [43]



(a)

(b)

Figure 4. Wire rope isolator (a) wire rope isolator installed in data communication system and (b) dimension of wire rope isolator

**2.3. Vibration tools**

The vibration test equipment primarily consists of five components: control computer, vibration controller, amplifier, electrodynamic shaker, and accelerometer. The vibration controller functions as a signal generator to drive the shaker. The amplifier will amplify the signal generated from the vibration controller to turn on the shaker according to the desired signal conditions. Acceleration transducers are used as measurements devices that provide inputs to the vibration controller. The accelerometers provide a feedback signal to the control computer. Figure 5 shows the basic components of an electrodynamic vibration testing system. For the placement of RX rocket data communication system that has been installed wire rope isolator and equipped with a tube on the vibration test machine can be seen in Figure 6.

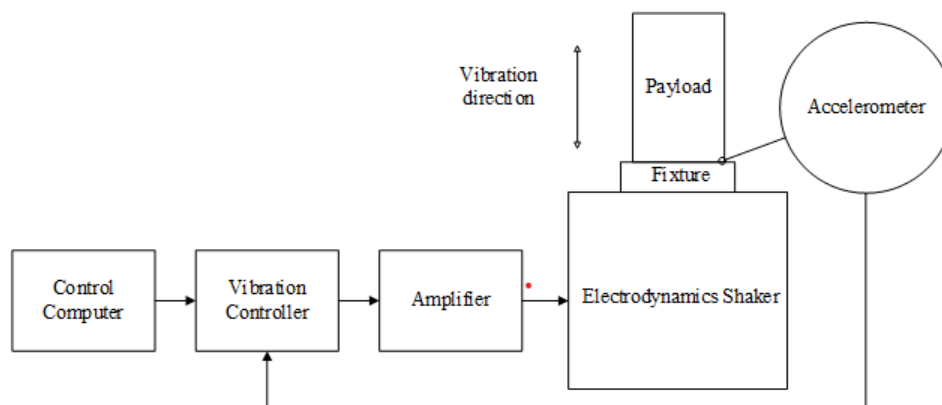


Figure 5. Basic components of an electrodynamic vibration testing system



Figure 6. Payload mounted in vibration test machine

### 3. RESULTS AND DISCUSSION

To design a large, high-performance sounding rocket, key considerations include achieving high acceleration, providing substantial initial thrust, and incorporating effective vibration and shock dampening systems. This study investigates the integration of four WRIs within the RX rocket's data communication compartment, arranged in a compressive configuration and aligned to optimize vibration attenuation. This setup aims to mitigate vibrations encountered during both ground-based vibration tests and in-flight test. While earlier studies have explored WRI systems, they have not explicitly addressed its influence on data communication systems on sounding rocket.

The method proposed in this research utilizes WRI dimensions, as shown in Figure 4, resulting in a WRI stiffness value consistent with calculated results. Specifically, the WRI stiffness is lower than the calculated maximum allowable stiffness (WRI stiffness < calculated maximum stiffness). The characteristics of the damper considered are the static load ( $W$ ), deflection ( $D$ ), and shock stiffness ( $Ks$ ) [42]. With a load mass of 30 kg, the total supported load data is obtained as follows:  $Wt = m \times g = 30 \text{ kg} \times 9,81 \text{ m/s}^2 = 294,3 \text{ N}$ . The number of WRI used is 4 units ( $n$ ), so the static load per isolator ( $W$ ) is  $Wt/n = 294,3/4 = 73,58 \text{ N}$ . The rocket propulsion operates by generating an excitation frequency of :  $fi = 93,3 \text{ Hz}$ . The system response natural frequency for 80% isolation is  $fn = fi/3 = 93,3/3 = 31,1 \text{ Hz}$  and the maximum isolator vibration stiffness ( $Kv$ ) is  $Kv = 73,58 \text{ N} \times \frac{2\pi fn^2}{g} = 286 \text{ kN/m}$ . After calculating the load per damper ( $W$ ) and the maximum damper stiffness ( $Kv$ ), both parameters are compared with the maximum static load that the damper can support and the actual damper stiffness under the conditions: Calculated  $W < \text{maximum damper static load} = 73,58 \text{ N} < 80 \text{ N}$  and WRI stiffness < calculated maximum stiffness ( $Kv < \text{calculated } Kv = 22 \text{ kN/m} < 286 \text{ kN/m}$ ). Our findings provide conclusive evidence that the vibration phenomenon that occurs on the RX rocket can be damped through the installation of WRI on a data communication system that weighs 30 kg.

#### 3.1. Vibration test

The testing process begins by powering on the vibration machine, the frequency measuring instrument, and the rocket's data communication system as shown in Figure 5. The test was performed by gradually increasing and decreasing the frequency to observe dynamic acceleration data. The frequency range used started from 0 Hz up to 2 kHz. Figure 7 shows the vibration test results recorded by the frequency measurement system installed on the vibration machine. Vibration testing was performed under two conditions: constant sweep vibration and random vibration. Figure 7 presents the results of the constant sweep vibration test on the vibration machine, conducted at frequencies ranging from 4 Hz to 600 Hz. The test started with an excitation of 1 g and went up to a maximum of 8 g. The graph shows no difference between the excitation input and the control accelerometer readings.

Figure 8 shows random vibration test result. In high frequency, vibration level obtained was  $0.4 \text{ G}^2/\text{Hz}$  while excitation of  $0.03 \text{ G}^2/\text{Hz}$  while at frequency 900 Hz and  $1 \text{ G}^2/\text{Hz}$  while excitation of  $0.04 \text{ G}^2/\text{Hz}$  at frequency 1600 Hz. The power system for the data communication system was turned on at the start of the vibration testing to record acceleration data from the sensors installed in the RX rocket's data communication system. The acceleration data from the rocket's data communication system is shown in



Figure 9. During the constant sweep vibration test, the recorded acceleration values were 8.37 g in Figure 9(a) and 8 g in Figure 9(b). In the random vibration test, the acceleration values were 20.37 g in Figure 9(c) and 8 g in Figure 9(d). The consistent recording of acceleration data by the sensors in the rocket's data communication system during the vibration test is attributed to the WRIs installed in the data communication compartment, which effectively dampened vibrations and shocks within the frequency range of 0 Hz to 1500 Hz.

The higher "g" readings on the test object sensor compared to the vibration machine readings are usually caused by phenomena such as resonance, differences in dynamic response, non-linear behavior, sensor placement location, and the swing effect when the vibration machine oscillates. This is the natural mechanical response to external vibrations during testing. However, despite the higher g-values received by the communication system's IMU compared to the vibration machine's maximum, the communication system continued to function correctly and transmitted signals without interruption or system shutdown, indicating that the WRI damping system performed adequately.

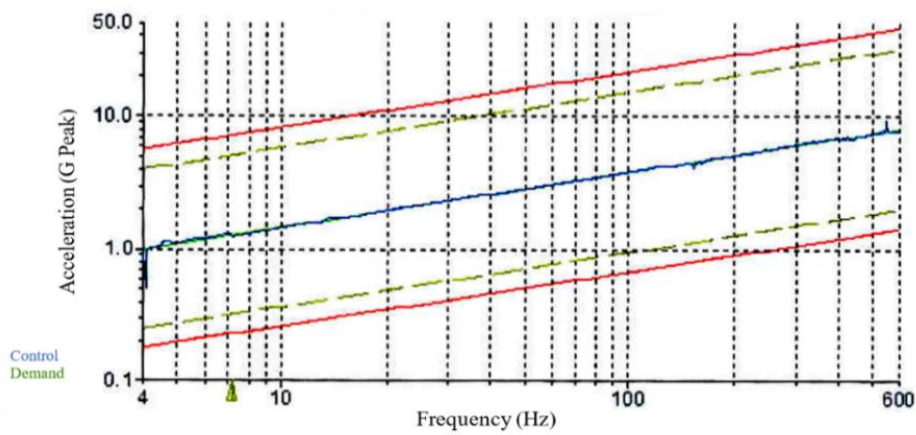


Figure 7. Acceleration data from the vibration machine at constant sweep vibration test

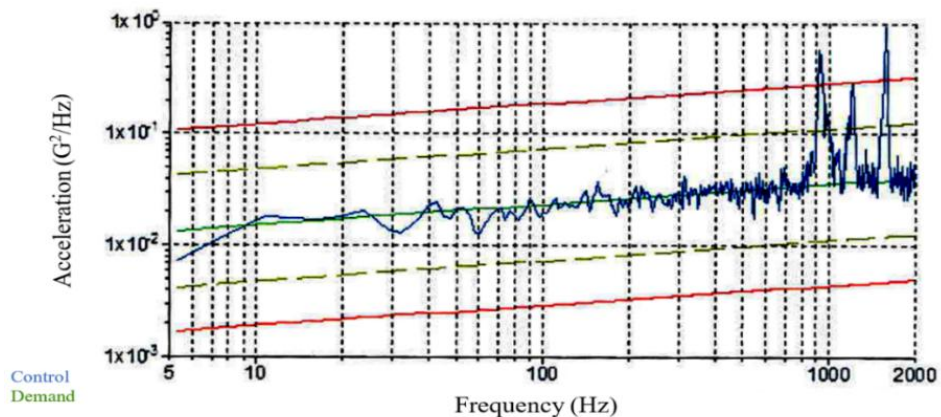


Figure 8. Acceleration data from the vibration machine during the random vibration test

### 3.2. Flight test

Based on the RX rocket flight test data received on the GCS, the performance of the stainless steel WRIs installed in the rocket's data communication system can be analyzed. Figure 10 shows the acceleration data obtained during the flight test, which reached 8 g and 9.3 g. Based on the vibration test results, the acceleration values of 8 g to 12 g occurred at frequencies between 800 Hz and 1500 Hz. This correlation between acceleration and frequency in the vibration test and the rocket flight test demonstrates that the wire rope isolators installed in the data communication compartment were able to dampen vibrations and shocks experienced during the rocket's launch from the pad.

To further improve the performance, especially in complex flight conditions, alternative damper configurations need to be explored in future research. The swing effect will be a reference factor for the selection of the position of the ballistic rocket damper in the next study. There are several positions that can be applied to the placement of the WRI position, namely the position of the reducer 45° compression/roll, fixed shear and fixed roll.

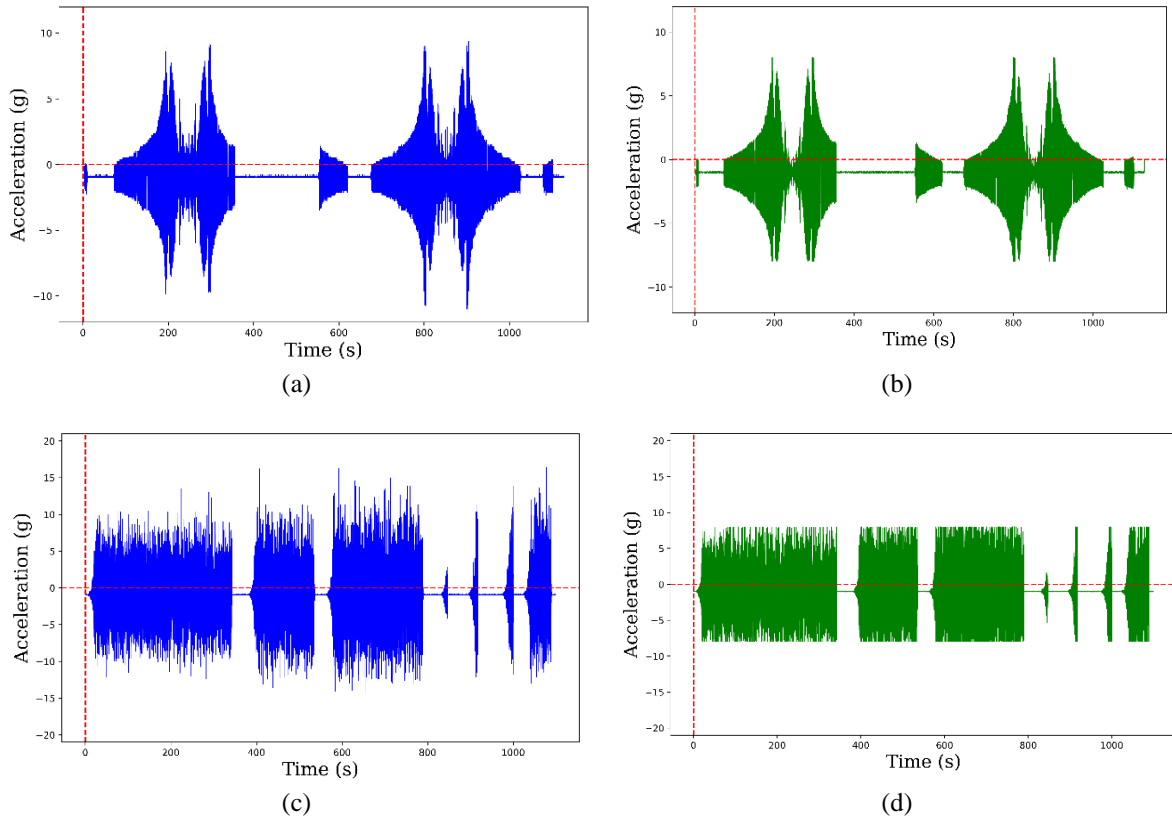


Figure 9. Acceleration data from communication data system on rocket RX: (a) acceleration data on constant sweep vibration test conditions 50 g, (b) acceleration data on constant sweep vibration test conditions 8 g, (c) acceleration data under random vibration test conditions 50 g, and (d) acceleration data under random vibration test conditions 8 g

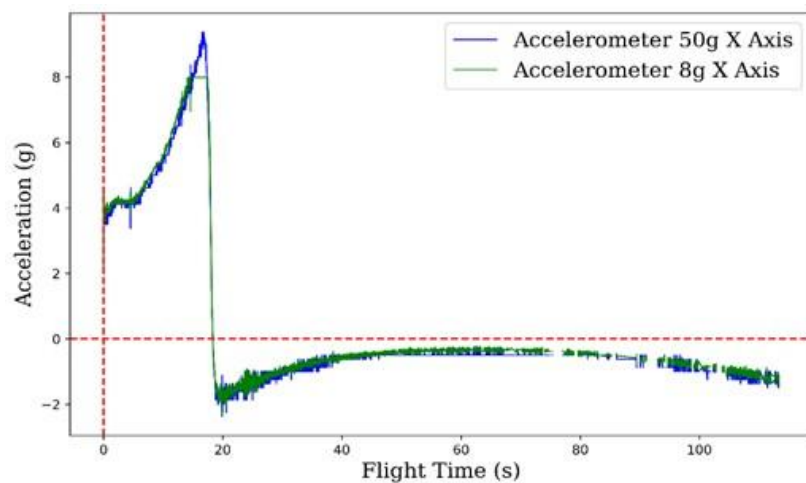


Figure 10. Acceleration data from communication data system on rocket test flight



#### 4. CONCLUSION

The data communication system of the RX ballistic rocket requires a reliable data communication system capable of withstanding severe vibrations and shocks during flight. This study demonstrates the effectiveness of WRI in reducing vibration and shock in a 30 kg rocket data communication system. Using 4 WRI units with a stiffness of 286 kN/m and total static load of 294.3 N, WRIs can withstand accelerations of up to 9.37 g during flight test and 12 g during vibration test, and ensuring stable data transmission to GCS. Although the mounting orientation and the number of dampers meet the requirements there are other external variables that arise such as swing effects. This swing effect causes a shift in the acceleration value of the rocket data communication with vibration device acceleration of  $\pm 1$  g.




#### REFERENCES

- [1] R. P. G. Collinson, *Introduction to avionics systems*. Dordrecht: Springer Netherlands, 2011.
- [2] W. Liu *et al.*, "The high-efficiency design method for capacitive MEMS accelerometer," *Micromachines*, vol. 14, no. 10, 2023, doi: 10.3390/mi14101891.
- [3] W. Yuan, "Development and application of high-end aerospace MEMS," *Frontiers of Mechanical Engineering*, vol. 12, no. 4, pp. 567–573, 2017, doi: 10.1007/s11465-017-0424-3.
- [4] D. R. Sparks, S. C. Chang, and D. S. Eddy, "Application of MEMS technology in automotive sensors and actuators," in *Proceedings of the International Symposium on Micromechanics and Human Science*, 1998, pp. 9–15, doi: 10.1109/mhs.1998.745744.
- [5] A. E. Stott, C. Charalambous, T. J. Warren, and W. T. Pike, "Full-band signal extraction from sensors in extreme environments: The NASA InSight microseismometer," *IEEE Sensors Journal*, vol. 18, no. 22, pp. 9382–9392, 2018, doi: 10.1109/JSEN.2018.2871342.
- [6] M. Bao and W. Wang, "Future of microelectromechanical systems (MEMS)," *Sensors and Actuators, A: Physical*, vol. 56, no. 1–2, pp. 135–141, 1996, doi: 10.1016/0924-4247(96)01274-5.
- [7] S. Saadon and O. Sidek, "A review of vibration-based MEMS piezoelectric energy harvesters," *Energy Conversion and Management*, vol. 52, no. 1, pp. 500–504, 2011, doi: 10.1016/j.enconman.2010.07.024.
- [8] Y. Ding, T. Xu, O. Onyilagha, H. Fong, and Z. Zhu, "Recent advances in flexible and wearable pressure sensors based on piezoresistive 3D monolithic conductive sponges," *ACS Applied Materials and Interfaces*, vol. 11, no. 7, pp. 6685–6704, 2019, doi: 10.1021/acsami.8b20929.
- [9] J. Hwang, Y. Kim, H. Yang, and J. H. Oh, "Fabrication of hierarchically porous structured PDMS composites and their application as a flexible capacitive pressure sensor," *Composites Part B: Engineering*, vol. 211, 2021, doi: 10.1016/j.compositesb.2021.108607.
- [10] X. Jiang, K. Kim, S. Zhang, J. Johnson, and G. Salazar, "High-temperature piezoelectric sensing," *Sensors (Switzerland)*, vol. 14, no. 1, pp. 144–169, 2014, doi: 10.3390/s140100144.
- [11] R. Margasahayam, R. Caimi, and J. Nayfeh, "Rocket launch-induced vibration and ignition overpressure response," pp. 1–8, 2019.
- [12] K. Wojciechowski, H. Graczyk, M. Piwowarczyk, R. Truszkowski, and P. Rękawek, "Data acquisition unit for suborbital rocket vibration measurement," *Journal of Physics: Conference Series*, vol. 2526, no. 1, 2023, doi: 10.1088/1742-6596/2526/1/012064.
- [13] E. Szpakowska-Peas and M. Krawczyk, "Selected problems of electronic equipment design in rocketry," *Transactions of the Institute of Aviation*, vol. 245, no. 4, pp. 209–217, 2016, doi: 10.5604/05096669.1226892.
- [14] Z. Ge, Y. Li, and S. Ma, "Attitude stabilization of rocket elastic vibration based on robust observer," *Aerospace*, vol. 9, no. 12, 2022, doi: 10.3390/aerospace9120765.
- [15] D. Adair, A. Nagimova, and M. Jaeger, "Effect of thrust on the structural vibrations of a nonuniform slender rocket," *Mathematical and Computational Applications*, vol. 25, no. 29, pp. 1–13, 2020, doi: 10.3390/mca25020029.
- [16] A. Okninski, B. Marciniak, B. Bartkowiak, and D. Kaniewski, "Development of the polish small sounding rocket program acta astronautica development of the polish small sounding rocket program," *Acta Astronautica*, vol. 108, pp. 46–56, 2015.
- [17] A. Dąbrowski and S. Krawczuk, "Analysis of a mechanical vibration filter and amplifier for sounding rocket applications," Jul. 2021, doi: 10.20944/preprints202107.0056.v1.
- [18] P. S. Balaji, M. E. Rahman, L. Moussa, and H. H. Lau, "Wire rope isolators for vibration isolation of equipment and structures-a review," in *IOP Conference Series: Materials Science and Engineering*, 2015, vol. 78, no. 1, doi: 10.1088/1757-899X/78/1/012001.
- [19] D. F. Ledezma-Ramírez, P. E. Tapia-González, M. J. Brennan, and P. J. Paupitz Gonçalves, "An experimental investigation into the shock response of a compact wire rope isolator in its axial direction," *Engineering Structures*, vol. 262, 2022, doi: 10.1016/j.engstruct.2022.114317.
- [20] C. Y. Zhou and T. X. Yu, "Analytical models for shock isolation of typical components in portable electronics," *International Journal of Impact Engineering*, vol. 36, no. 12, pp. 1377–1384, 2009, doi: 10.1016/j.ijimpeng.2009.03.013.
- [21] M. E. Danowski *et al.*, "Vibration isolation design for the micro-x rocket payload," *Journal of Low Temperature Physics*, vol. 184, no. 3–4, pp. 597–603, 2016, doi: 10.1007/s10909-016-1580-2.
- [22] M. Leblouba, P. S. Balaji, and M. E. Rahman, "Wire rope isolators for the vibration protection of heavy equipment: Exploratory research," *Buildings*, vol. 12, no. 12, 2022, doi: 10.3390/buildings12122212.
- [23] H. Dal and M. Baklaci, "The effect of wire rope material on vibration characteristics," *European Journal of Engineering Science and Technology*, vol. 4, no. 1, pp. 15–26, 2021, doi: 10.33422/ejest.v4i1.608.
- [24] D. F. L. Ramirez, P. E. Tapia Gonzalez, M. Castillo Morales, T. P. Berber Solano, and A. Salas Zamarripa, "Shock response of a two-stage vibration isolation system," *Ingeniería Investigación y Tecnología*, vol. 21, no. 2, pp. 1–11, 2020, doi: 10.22201/i.25940732e.2020.21n2.018.
- [25] U. Ferdek and M. Dukała, "Experimental analysis of nonlinear characteristics of absorbers with wire rope isolators," *Open Engineering*, vol. 11, no. 1, pp. 1170–1179, 2021, doi: 10.1515/eng-2021-0111.
- [26] M. L. Tinker and M. A. Cutchins, "Damping phenomena in a wire rope vibration isolation system," *Journal of Sound and Vibration*, vol. 157, no. 1, pp. 7–18, 1992, doi: 10.1016/0022-460X(92)90564-E.
- [27] M. Guzmán-Nieto, P. E. Tapia-González, and D. F. Ledezma-Ramírez, "Low frequency experimental analysis of dry friction damping in cable isolators," *Journal of Low Frequency Noise Vibration and Active Control*, vol. 34, no. 4, pp. 513–524, 2015, doi: 10.1260/0263-0923.34.4.513.




- [28] P. E. Tapia-González and D. F. Ledezma-Ramírez, "Experimental characterisation of dry friction isolators for shock and vibration," *Journal of Low Frequency Noise Vibration and Active Control*, vol. 36, no. 1, pp. 83–95, 2017, doi: 10.1177/0263092317693509.
- [29] D. Pellicchia, N. Vaiana, M. Spizzuoco, G. Serino, and L. Rosati, "Axial hysteretic behaviour of wire rope isolators: Experiments and modelling," *Materials and Design*, vol. 225, Jan. 2023, doi: 10.1016/j.matdes.2022.111436.
- [30] D. F. Ledezma-Ramírez, P. E. Tapia-González, N. Ferguson, M. Brennan, and B. Tang, "Recent advances in shock vibration isolation: An overview and future possibilities," *Applied Mechanics Reviews*, vol. 71, no. 6, 2019, doi: 10.1115/1.4044190.
- [31] K. Lai, W. Fan, Z. Chen, C. Yang, Z. Liu, and S. Li, "Performance of wire rope damper in vibration reduction of stay cable," *Engineering Structures*, vol. 278, 2023, doi: 10.1016/j.engstruct.2022.115527.
- [32] M. W. Beranek, "Fiber optic interconnect and optoelectronic packaging challenges for future generation avionics," in *Proceedings of SPIE - The International Society for Optical Engineering*, 2007, vol. 6478, pp. 111–128, doi: 10.1117/12.709761.
- [33] M. Montesarchio, A. L. Zollo, M. Ferrucci, and E. Bucchignani, "Latest developments in AWAS: The advanced weather awareness system in the COAST project," in *IOP Conference Series: Materials Science and Engineering*, 2022, vol. 1226, no. 1, pp. 1–8, doi: 10.1088/1757-899x/1226/1/012089.
- [34] V. Di Vito, P. Grzybowski, T. Rogalski, and P. Maslowski, "Design advancements for an integrated mission management system for small air transport vehicles in the COAST project," *Aircraft Engineering and Aerospace Technology*, vol. 94, no. 9, pp. 1508–1516, 2022, doi: 10.1108/AEAT-02-2022-0038.
- [35] C. Zhang, X. Shi, and D. Chen, "Safety analysis and optimization for networked avionics system," in *2014 IEEE/AIAA 33rd Digital Avionics Systems Conference (DASC)*, 2014, pp. 1–17, doi: 10.1109/dasc.2014.6979613.
- [36] N. Silva and L. G. Trabasso, "IMFLAR: An intuitive method for logical avionics reliability," *Journal of Aerospace Technology and Management*, vol. 5, no. 1, pp. 111–126, 2013, doi: 10.5028/jatm.v5i1.165.
- [37] G. Xiao, Y. Wang, and F. He, "Research on safety modeling and analysis in information fusion system," *Aerospace Systems*, vol. 2, no. 1, pp. 51–60, 2019, doi: 10.1007/s42401-018-0011-2.
- [38] S. R. Girard, V. Legault, G. Bois, and J. F. Boland, "Avionics graphics hardware performance prediction with machine learning," *Scientific Programming*, vol. 2019, 2019, doi: 10.1155/2019/9195845.
- [39] J. Xu and L. Xu, "Integrated system health management-based condition assessment for manned spacecraft avionics," *Journal of Aerospace Engineering*, vol. 227, no. 1, pp. 19–32, 2013, doi: 10.1177/0954410011431395.
- [40] G. Qi, R. Duan, H. Sun, H. Zhou, Z. Xiang, and W. Li, "Next generation avionics system of future launch vehicle," in *Joint International Mechanical, Electronic and Information Technology Conference*, 2015, pp. 1215–1219, doi: 10.2991/jimet-15.2015.230.
- [41] K. Rahardiyanti *et al.*, "Design and testing of data communication system integration on RX-450.03 sounding rocket," in *2023 IEEE Asia-Pacific Geosciences, Electronics and Remote Sensing (AGERS)*, 2023, pp. 34–42, doi: 10.1109/AGERS61027.2023.10490808.
- [42] S. Wang, X. Li, S. Lei, J. Zhou, and Y. Yang, "Research on torsional fretting wear behaviors and damage mechanisms of stranded-wire helical spring," *Journal of Mechanical Science and Technology*, vol. 25, no. 8, pp. 2137–2147, 2011, doi: 10.1007/s12206-011-0532-7.
- [43] ENIDINE, "Wire rope isolator technologies applications." Online.] Available: [https://www.enidine.com/getmedia/a2281e2d-5291-4c64-941c-84ce4d3659ba/WR\\_Catalog.pdf](https://www.enidine.com/getmedia/a2281e2d-5291-4c64-941c-84ce4d3659ba/WR_Catalog.pdf) (Accessed: Dec. 31, 2024)

## BIOGRAPHIES OF AUTHORS






**Kandi Rahardiyanti**    completed her Bachelor's degree from Institute Teknologi Sepuluh Nopember, Surabaya, Indonesia, in 2011 and her Master degree from Universitas Indonesia, Depok, Indonesia, in 2021, respectively in electrical engineering. Since 2014, she has been an engineering staff at Rocket Technology Center, National Research and Innovation Agency. She can be contacted at email: kand001@brin.go.id.



**Shandi Prio Laksono**    received his Bachelor's degree from Bandung Institute of Technology in 2011, majoring in Mechanical Science And Engineering. In 2014, he joined the Research Center for Rocket Technology. Since 2020, he has obtained his master's degree from Kanazawa University, Japan. Currently, he is a researcher at the Research Center for Energy Conversion and Conservation. His research activities include designing, modeling, and simulating new and renewable energy. He can be contacted at email: shan002@brin.go.id.






**Khaula Nurul Hakim**    completed his Bachelor's degree of in Electronics And Instrumentation from Gadjah Mada Universtiy, Yogyakarta, Indonesia, in 2013 and his Master degree in Electronics And Electrical Engineering from Keimyung University, Daegu, South Korea in 2020. He worked as an engineering staff at avionic system for rocket power management and as a member of dynamic sensor lab for payload system in Rocket Technology Center (2014-2022). Since 2022, he has been working as an engineering staff in Research Centre for Electronics in the National Research and Innovation Agency. He can be contacted at email: khau001@brin.go.id.






**Yuniarto Wimbo Nugroho**    completed his Bachelor's degree of Applied Science in Electronic Engineering from State Polytechnic of Bandung, and received his Master degree in Electronic And Electrical Engineering from Keimyung University, Daegu, South Korea in 2020. Since 2015, he has worked as an engineer at Rocket Technology Center, National Research and Innovation Agency of Republic Indonesia (BRIN), Bogor, Indonesia. His main research interest are focusing on control engineering, sensors, and artificial intelligence. He can be contacted at email: yuni019@brin.go.id.






**Andreas Prasetya Adi**    received his Bachelor's and Master degree of Engineering in Computer Science from Gunma University, Japan, in 1995 and 1997, respectively. Since 1997 he has been a researcher at the Rocket Technology Center, National Institute of Aeronautics and Space (LAPAN). Since 2022 he is with the Research Center of Aeronautics Technology, National Research and Innovation Agency (BRIN). He can be contacted at email: andr006@brin.go.id.



**Salman**    completed his Bachelor's degree in Electronic Engineering from Islamic University of Indonesia, Yogyakarta, in 2008. He worked as a research assistant in PUSTEKROKET LAPAN from 2009-2021. He is presently works as an engineering staff at Innovation and Product Development Division for Ammunition at PT. Pindad. He can be contacted at email: salman.kyn@gmail.com.



**Kurdianto**    received the M.Eng degrees electrical engineering from Beihang University, Beijing, China in 2014. The author is a researcher at the National Institute of Aeronautics and Space (LAPAN) who served at the rocket technology center until 2021. In 2022 as a researcher at the National Research and Innovation Agency (BRIN) in charge of the Research Center of Geoinformatics. He is also a member of the Indonesian researchers Association (Himpenindo) until 2021 and in 2022 as a member of the Indonesian researchers Association (PPI). He can be contacted at email: kurd001@brin.go.id.